Journal of Magnetic Resonance **157,** 141–155 (2002)
doi:10.1006/jmre.2002.2570

Towards Rapid and Unique Curve Resolution of Low-Field NMR Relaxation Data: Trilinear SLICING versus Two-Dimensional Curve Fitting

Henrik Toft Pedersen, Rasmus Bro, and Søren Balling Engelsen[1]

Centre for Advanced Food Studies, Department of Dairy and Food Science, Food Technology, The Royal Veterinary and Agricultural University, Rolighedsvej 30, DK-1958 Frederiksberg C, Denmark

Received April 5, 2002

In this work an alternative method, named SLICING, for two-dimensional and noniterative T_2 decomposition of low-field pulsed NMR data (LF-NMR) is proposed and examined. The method is based on the Direct Exponential Curve Resolution Algorithm (DECRA) proposed by W. Windig and A. Antalek (1997, *Chemom. Intell. Lab. Syst.* 37, 241–254) and takes advantage of the fact that exponential decay functions, when translated in time, retain their characteristic relaxation times while only their relative amounts or concentrations change. By such simple translations (slicing) it is possible to create a new "pseudo" direction in the relaxation data and thus facilitate application of trilinear (multiway) data-analytical methods. For the application on LF-NMR relaxation data, the method has two basic requirements in practice: (1) two or more samples must be analyzed simultaneously and (2) all samples must contain the same qualities (i.e., identical sets of distinct T_2 values). In return, if these requirements are fulfilled, the SLICING (trilinear decomposition) method provides very fast and unique curve-resolution of multiexponential LF-NMR relaxation curves and, as a spin-off, calibrations to reference data referring to individual proton components require only scaling of the resulting unique concentrations. In this work the performance of the SLICING method (including multiple slicing schemes) is compared to a traditional two-dimensional curve fitting algorithm named MATRIXFIT through application to simulated data in a large-scale exhaustive experimental design and the results validated by application to two small real data sets. Finally a new algorithm, Principal Phase Correction (PPC) based on principal component analysis, is proposed for phase rotation of CPMG quadrature data, an important prerequisite to optimal SLICING analysis. © 2002 Elsevier Science (USA)

Key Words: **low-field ^{1}H NMR; DECRA; DTLD; transverse relaxation; T_2 relaxation; exponential decay; meat; curve fitting.**

INTRODUCTION

Low-field ^{1}H pulsed NMR (LF-NMR) is a direct and exciting technology for probing proton mobility in, e.g., food and feed. The importance of such a probe cannot be overestimated due to the fundamental impact on food quality of the physics of the two major proton-carrying components: fat and water. The hydration characteristics of food and feed determine to a great extent its oxidative behavior, as water is the carrier medium of most oxidation processes including microbiological processes. The overall water compartmentalization will often mirror the basic food structure and thus indirectly or directly reflect rheological and sensory quality attributes. Fat content and solid fat index are quality attributes of prime importance to the nutritional character of the food and to the mouth feel, respectively. LF-NMR has the potential not only to measure all of these important food quality attributes but also to perform the task as a noninvasive volumetric measure. While LF-NMR does not suffer from limitations in possible pulse and field gradient applications, it suffers from a crude resolution and is normally only recorded and analyzed in the time domain.

In the time domain, transverse LF-NMR relaxation data are assumed to be a sum of exponentials,

$$\mathbf{x}(\mathbf{t}) = \sum_{n=1}^{N} M_n \cdot \exp\left(\frac{-\mathbf{t}}{T_{2n}}\right) + \mathbf{e}, \qquad [1]$$

where $\mathbf{x}$ is a J-vector holding the acquired data for a single sample, N is the number of exponential functions or components in the sample, M_n is the concentrations or amplitudes of the nth exponentials, T_{2n} is the corresponding relaxation time constants, $\mathbf{t}$ is the acquisition time axis, and $\mathbf{e}$ is the residual error. While the T_2's provide a qualitative description of the spin–spin relaxation, the M_n holds the quantitative description. Normally transverse LF-NMR relaxation curves obey Eq. [1], but a number of physical sample effects as described by Diegel and Pintar (*2*) and Köpf *et al.* (*3*) as well as instrumental effects may give rise to nonexponential lineshapes.

Two fundamentally different data analytical strategies can be applied to analyze instrumental multivariate colinear data such as NMR spectra and relaxation decays: (I) one-dimensional analysis in which the data structures from each sample are analyzed individually and (II) two-dimensional analysis in which a

[1] To whom correspondence should be addressed. E-mail: se@kvl.dk.

1090-7807/02 $35.00

series of related data structures are analyzed simultaneously. For exponentially decaying relaxation curves the one-dimensional data analytical approach has two well-established forms:

(1) *Discrete exponential fitting.* In this classical approach, the relaxation profiles are individually decomposed into a limited number of pure exponential curves (typically less than 5). This is the classical approach and scientists working in the numerical field have been struggling with and refining it for more than 200 years (*4*). More recent numerical approaches include quasi-Newton least squares fitting using soft line search and factorization. Despite the ill-conditioning property of the exponential-sum fitting problem, in practice numerical methods have become fairly robust, but unfortunately the iterative methods are rather time-consuming. More importantly, the final results are often strongly dependent on the number of exponential components extracted.

(2) *Distributed exponential fitting.* Distribution analysis is the natural generalization of the oligo-exponential analysis where the relaxation curve is least squares fitted to a continuous distribution of characteristic relaxation times (exponentials) (*5, 6*). This approach is appealing to scientists working with interpretation of NMR relaxation profiles, as relaxation components are generally considered as having relatively large variation in their T_2 values. However, if the results of distributed exponential fitting and discrete exponential fitting for a given sample are compared, it is often seen that the time constants of the discrete analysis coincide with the modes of the peaks in the continuous analysis. For this reason, exponential fitting does, in fact, reveal useful information about the origin of protons in the sample. Mathematically speaking, the distributed exponential fitting problem is ill-posed, for which reason its numerical solution requires regularization. Even with regularization, results from current algorithms do not converge convincingly and are exceedingly slow.

The two-dimensional methods are generally more robust and require fewer assumptions about the data structure. For NMR time-domain relaxation curves the two-dimensional quantitative data analytical approach has a minimum of two forms:

(3) *Discrete exponential matrix fitting* (MATRIXFIT). This is the two-dimensional analogue to the discrete exponential fitting, in which several relaxation decays are analyzed simultaneously assuming that the qualities remain unchanged. In this approach M_n is a vector of amplitudes with I elements and T_{2n} are common time constants for all I samples. The entire set of relaxation decays is thus fitted at the same time to a common set of underlying exponentials.

(4) *Bilinear multivariate data analysis (chemometrics).* In recent years chemometric methods have been applied for analysis of LF-NMR data (*7–10*). The essence of most chemometric methods lies in their construction of common latent factors (or principal components) from underlying latent structures in the original data from many samples. The mathematical model for this problem can be described as

$$\mathbf{X} = \mathbf{T} \cdot \mathbf{P}^{\mathrm{T}} + \mathbf{E}, \qquad [2]$$

where $\mathbf{X}$ is the transverse LF-NMR data matrix ($I \times J$; one relaxation profile per row), $\mathbf{P}$ contains the underlying profiles ($J \times N$; loadings), and $\mathbf{T}$ is the contributing amplitudes ($I \times N$; scores). The scalar N is the number of factors resolved and $\mathbf{E}$ ($I \times J$) holds residual unexplained variation. Chemometric data analysis has proven to perform well especially in quantitative calibration problems and to be extraordinarily robust when applied to LF-NMR data. The disadvantage of using chemometric models is that it requires data from many samples to be analyzed simultaneously and the qualitative information (time constants) is lost due to the common practice of extracting orthogonal latent factors. However, in certain cases where the data from each sample are two-dimensional, such as in excitation-emission fluorescence spectra, trilinear chemometric methods that can resolve the underlying non-orthogonal factors uniquely (*vide supra*) are available.

In this work we will describe, test, and discuss a new 2D algorithm for the analysis of LF-NMR data that may be considered as a combination of the best features from (1) and (4), but its solution ideally should be identical to (3). The novel approach is to upgrade a one-dimensional relaxation curve to become a pseudo two-dimensional structure and thus facilitate the unique advantages offered by trilinear models. The method is basically built on the fact that two different time "slices" (Fig. 1) of a given multiexponential decay curve consist of the same underlying features (**quality**, characteristic decay times), but in a new linearly related combination of amounts (**quantity**, concentrations or magnitudes). Windig and Antalek (*1*) originally conceived the idea and proposed a fast alternative to the trilinear least squares solution, which they called the Direct Exponential Curve Resolution Algorithm (DECRA). In other words the new approach is built on the linear relationship between exponentials,

$$\exp\left(\frac{-\mathbf{t}}{T_{2n}}\right) \propto \exp\left(\frac{-\mathbf{t} + \Delta\mathbf{t}}{T_{2n}}\right) \qquad [3]$$

and similar ideas have also appeared in telecommunication under the generic name ESPRIT (*11–13*). In their first application, Windig and Antalek applied the method to perform exponential curve resolution of first-order reaction kinetics ($C = C_0 \cdot \mathrm{e}^{-\mathrm{k}\cdot\mathrm{t}}$) as monitored by high-resolution NMR at the process line at KODAK (U.S.). Since the first publication of DECRA, several authors have applied the algorithm or modifications of it in a series of applications such as multivariate image analysis based on magnetic resonance images (*14–17*) short-wavelength near infrared analysis (*18*), UV-VIS (*19, 20*), and solid state NMR and mid-infrared (*21*). Common to these applications is the step of generating the three-way data array based on a measured two-way matrix, whereas different algorithms are used to perform the deconvolution. Applications of DECRA reported so far have the

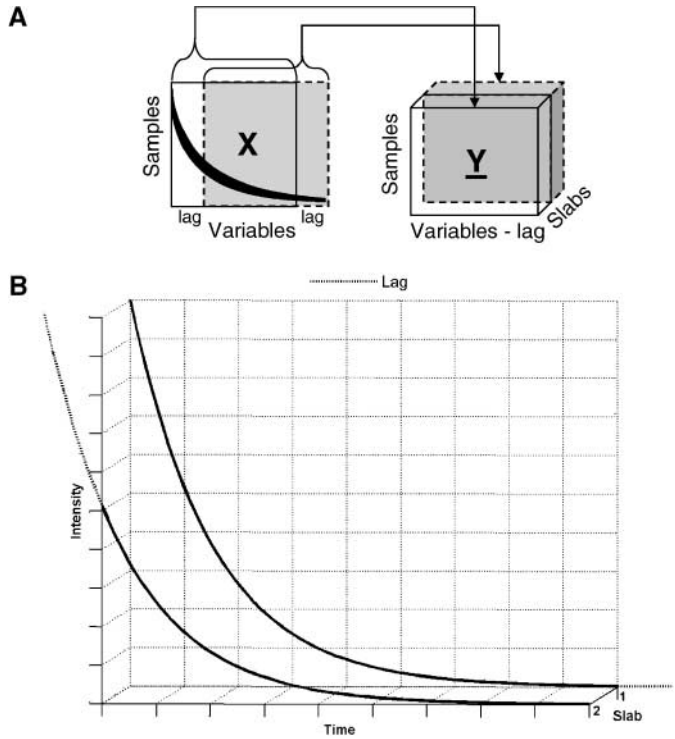

FIG. 1. (A) Illustration of the concept of rearranging a two-way data matrix into submatrices and placing them behind each other to create a new linear direction in the data, i.e., a three-way data structure. The figure shows the case where data have been lagged *lag* and two *slabs* are created. (B) Enlargements of the representation in (A) for a single sample to improve visualization.

direction of exponential decay between spectra (rows) that are recorded as time series of the same sample. Such applications, in which the sample has been left in the spectrometer throughout the measurements, are ideal sampling situations, increasing the sampling repeatability and thus eliminating a number of factors that might otherwise introduce noise and disturbances into the data. In this work, we propose and examine the combined use of Windig and Antalek's "slicing method" and trilinear methods to analyze low-resolution transverse relaxation decays that are multivariate exponential decay curves from a set of samples rather than a multivariate measurement on one sample as a function of time. The direction of exponentiality here is in the variable direction rather than in the sample direction, which gives rise to a few problems that, will be briefly outlined. The algorithm for analysis of transverse LF-NMR data suggested in this paper is based on the concept of the "slicing" rearranging data as described in DECRA, but a number of steps have been included in the deconvolution to improve the DECRA algorithm towards transverse LF-NMR relaxation data. The described algorithm, optimized to LF-NMR data, will be termed SLICING throughout this paper, in acknowledgement of the fact that data are sliced to produce the three-way array. At this point is should be stressed that the new algorithm as well as algorithms (1)–(3) are based on the assumption that the relaxation data exhibit "pure" multiexponential behavior. The aims of this study are to evaluate the performance of the new SLICING algorithm using different slicing principles including an optimized approach and a new uncorrelated approach and to compare their performances to the MATRIXFIT procedure. For this purpose a large-scale exhaustive experimental design of simulated data was constructed and finally the results were validated using two simple real datasets.

THEORY AND METHODS

In this section we will outline the algorithms used in this study with special emphasis on the new SLICING algorithm, but first the two-dimensional curve-fitting algorithm is briefly outlined.

MATRIXFIT

For this approach we have chosen a rather pragmatic approach which to excess has proven robust, reliable, and relatively rapid. The algorithm was originally written for one-dimensional multiexponential fitting as stated in Eq. [1], but the extension to performing multiexponential fitting on two-dimensional data is straightforward. Rather than optimizing the fit for one sample at the time the residual error of the optimization is calculated for the entire data matrix, we use a common time constant for all samples but with concentrations individual to each sample calculated by the fit. This way the time constants and concentrations that best describe the entire data matrix for a given number of components are calculated. In terms of Eq. [1] this implies that T_{2n} is identical to all samples and only M_n varies for each sample. An algorithm capable of similar two-dimensional multiexponential deconvolution called SPLMOD has previously been made available on the Internet in a Fortran compilation (22).

Trilinear Theory

Second-order low-rank trilinear data have the distinct advantage that they can be decomposed according to a so-called parallel factor analysis (PARAFAC) model (*23–25*). Approximate trilinear data follow the model

$$x_{imk} = \sum_{n=1}^{N} t_{in} p_{mn} s_{kn} + e_{imk}, \quad i = 1, \ldots, I; m = 1, \ldots, J; k = 1, \ldots, K. \qquad [4]$$

The data are held in the elements x_{imk}, the parameters t_{in} hold the so-called loadings pertaining to the first mode typically gathered in $\mathbf{T}$ ($I \times N$), p_{mn} holds the loadings pertaining to the second mode held in $\mathbf{P}$ ($M \times N$), s_{kn} holds the loadings pertaining to the third mode held in $\mathbf{S}$ ($K \times N$), and e_{imk} holds residual unexplained variation (see Fig. 2). The elements x_{imk} are held in a three-way $I \times M \times K$ array and are triply subscripted meaning that the data can be arranged in a three-way cube of data as opposed to ordinary doubly subscripted data corresponding to

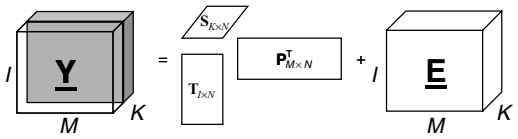

FIG. 2. Schematic drawing of a three-way array decomposed by a trilinear model. The dimension of the three-way array is I samples, M variables, and K *slabs*, and **T** represents the score matrix or concentrations, **P** is the exponential loadings or latent variables, and **S** is the *slab* mode loadings. N is the number of components deconvoluted.

a matrix. In bilinear modelling of matrices (e.g., principal component analysis—Eq. [2]) the parameters are only identified up to rotation unless *a priori* constraints such as, for example, unimodality and nonnegativity are applied. Thus, even though a set of several LF-NMR profiles follows the bilinear model, it is not possible to actually find the exponential profiles and their corresponding amplitudes because an infinity of solutions provides the same fit. For the PARAFAC model, however, the parameters are uniquely identified up to trivial scaling and permutation. Hence, if the data follow the model, the individual components can be identified directly (*25*).

For trilinear modelling, a number of different algorithms are available including Generalized Rank Annihilation Method (GRAM) (*26*) and Direct TriLinear Decomposition (DTLD) (*27*) which is a generalization of GRAM and PARAFAC-ALS (*23–25*). While the two former algorithms are based on a generalized eigenvalue problem and computationally relatively "inexpensive," they do not provide the least squares solution to the posed problem. For large data sets with high signal-to-noise ratio and little model error, the deviation from the least squares solution is usually insignificant. If, however, the least squares solution to the three-way problem is required, the PARAFAC-ALS algorithm is a suitable choice. PARAFAC-ALS has certain advantages, but being an iterative procedure it does not share the computational efficiency of the GRAM-based methods and will not be pursued here, since algorithmic speed is one of the primary goals. Application of GRAM-based algorithms is also reasonable due to properties of the problems typically solved with DECRA, since these are often based on precise measurements that closely follow the stipulated model. Also, it is important to keep in mind that since the data analytical problem initially is a two-way problem, a least squares solution to the three-way problem (and hence not to the two-way problem of Eq. [2]) is still no guarantee that the obtained solution is statistically optimal.

In this study it was desired to obtain a flexible algorithm that can deal with complex slicing schemes including multiple slices (see below) and as more than two *slices* are generated, GRAM can no longer be used, because GRAM intrinsically requires that the dimension is two in one of the modes. Direct trilinear decomposition (DTLD) is a generalization of GRAM that can handle multiple *slices* and was therefore chosen for this work (*27*). In the case of having only two *slices*, the solution calculated by DTLD is identical to the GRAM solution.

SLICING Procedures

If equitemporally measured transverse LF-NMR data from two or more samples can be approximated by

$$\mathbf{X} = \mathbf{T} \cdot \mathbf{P}_{\text{exp}}^{\text{T}}, \qquad [5]$$

where the $\mathbf{P}_{\text{exp}}$ contain N underlying profiles of length J ($J \times N$) which are distinct monoexponentials, then it can be shown that the data can be rearranged into a so-called three-way array $\underline{\mathbf{Y}}$ of size $I \times M \times K$ as depicted in Fig. 1A. If $\mathbf{X}$ has elements x_{ij}, ($i = 1, \ldots, I; j = 1, \ldots, J$), then the three-way array $\underline{\mathbf{Y}}$ can consist of two submatrices of dimension $I \times J - 1$, where the first submatrix contains the *first* $J - 1$ columns of $\mathbf{X}$ and the second submatrix contains the *last* $J - 1$ columns of $\mathbf{X}$. Hence, the major part of the two matrices will be identical, but shifted "horizontally" by a fixed amount. The submatrices in the resulting three-way array will be referred to as *slabs* and the number of columns to shift between the two *slabs* (in this case one) will be referred to as *lag*. The interpretation of *lag* and *slab* is displayed in Fig. 1A with a more detailed picture for only one sample in Fig. 1B. It can be shown that when the original data follow the model of Eqs. [1] and [5], then this three-way array will follow a trilinear model in which the parameters are related to the parameters in Eq. [4]. This property will be explained in detail later. This is important, because the PARAFAC model can be shown to be essentially unique under mild conditions (up to some trivial scaling and permutation indeterminacies that are intrinsic to the problem). This again implies that the parameters in Eq. [1] can be estimated directly from the PARAFAC model; i.e., the defining exponentials as well as their magnitudes in the different samples are found directly from the PARAFAC model. There are multiple slicing choices that can be made to achieve the pseudo upgrade of the bilinear data to fulfill the requirements of trilinear modelling. In this study we test and compare four different slicing schemes described below.

DECRA or SLICING$_{[1;2]}$

The original DECRA algorithm is based on GRAM and uses *lag* equal one and *slab* equal two (subindicies refer to [lag; slab]), i.e., the simplest three-way array possible to create from a two-way matrix by the "slicing" rearrangement. It should be stressed that the DECRA solutions referred to in this study are not identical to the original, as it uses the algorithmic scheme outlined below.

Multiple Odd-Spaced SLICING: SLICING$_{[1\text{-}10\text{-}100;3]}$ and SLICING$_{[1\text{-}5\text{-}10\text{-}50\text{-}100;5]}$

In practice, there is nothing to hinder *lagging* the data more than one variable, still maintaining two *slabs* (*19*) or leading

to possible generation of three or more *slabs* in the third mode (*20*). When the dimension of the third mode increases, the three-way array $\underline{\mathbf{Y}}$, with elements y_{imk}, will now have the dimension $i = 1, \ldots, I; m = 1, \ldots, J - L \cdot (K - 1); k = 1, \ldots, K$ with $2 \leq K \leq L + 1$ where L is the selected *lag* and K is the specified number of *slabs*.

A slightly more elaborate approach than DECRA is the generation of multiple odd-spaced slices. In this approach it is possible to specify that selected variables must be used to generate the different slabs. Two representative combinations with three and five slabs have been included in this study with the first variables in the three slabs being 1, 10, and 100 (refereed to as $\text{SLICING}_{[1\text{-}10\text{-}100;3]}$) and the first variables in the five slabs being 1, 5, 10, 50, and 100 (refereed to as $\text{SLICING}_{[1\text{-}5\text{-}10\text{-}50\text{-}100;5]}$). The rationale for selecting the variables to generate odd-spaced three-way structure is the desire to properly represent both short and long time constants which is expected to be improved in this way compared with the normal equidistant spacing being better for either short or long time constants depending on the value of *lag*.

$\text{SLICING}_{\text{OPT}}$

The determination of multiple and optimal *slab* and *lag* in SLICING has not yet been described mathematically and different applications provide ambiguous results. While Windig *et al.* (*21*) propose that a *lag* of one and thus only two *slabs* is the optimal solution, Bijlsma *et al.* (*19*) propose in another setting that a *lag* greater than one, even if only two *slabs* are used, improves the obtained result. In another study, Bijlsma and Smilde (*20*) investigate the use of both 3 and 4 *slabs*; however, no significant improvement over the two *slab* models is observed. Presumably, a number of parameters will influence the choices of optimal *lag* and *slab*, e.g., the noise level of the acquired data, the number of samples in the data set, the number of underlying monoexponential components (rank) in the system, and the degree to which the data follow the stipulated model. In the $\text{SLICING}_{\text{OPT}}$ scheme we investigate the optimal slicing scheme by examining the model error for a range of combinations of the two meta-parameters *lag* and *slab* to find the optimal *lag* and *slab* for a given number of factors to resolve (N).

Nonredundant SLICING

In this study a completely new approach for slicing the data in which the slabs use nonredundant information and which avoids correlated noise is evaluated. The main difference between this approach and the above "slicing" procedures is that the noise in the normal SLICING procedure noise is correlated between the different slabs since data are duplicated and reused to generate the three-way structure whereas in the new approach all data points in the three-way structure are unique and the noise is thus uncorrelated at least by construction.

The new approach is based on the fact that different slabs can be generated from different data points by letting the first variable followed by every xth variable span the first slab, the second variable followed by every xth variable span the second slab, and so forth. Following this syntax will result in x slabs and the total number of data points is maintained constant since no data are duplicated.

The SLICING Algorithm

In this study the different SLICING schemes have been implemented in an algorithmic procedure which in the case of $\text{SLICING}_{\text{OPT}}$ is displayed in Fig. 3 and will be outlined in some detail below. The best solution with monoexponential loadings

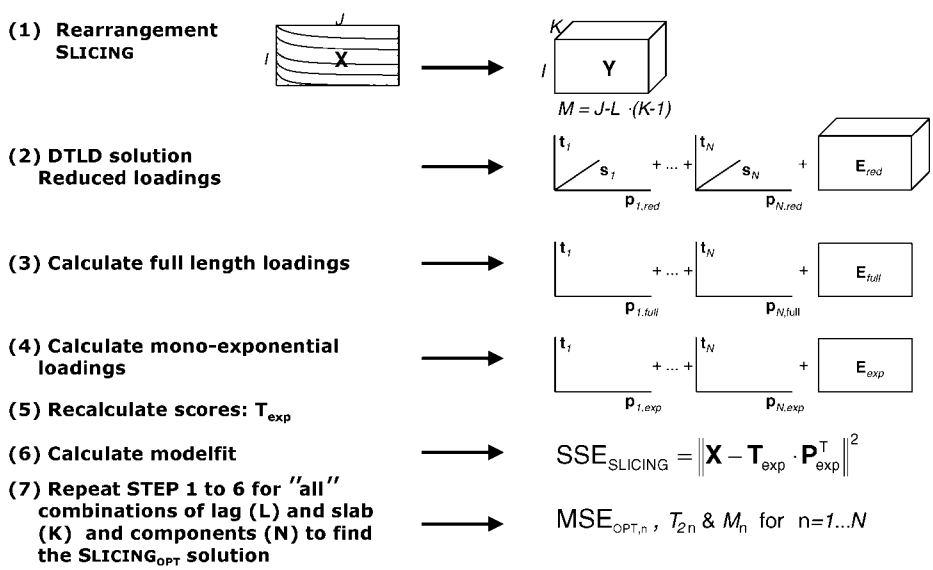

FIG. 3. Schematic figure of the steps involved in the SLICING algorithm.

is found through a number of steps. Step 1 is the rearrangement of the relaxation profiles according to the SLICING model described above. Step 2 is the deconvolution of the exponential decay profiles by DTLD using N factors. From the DTLD algorithm one score matrix ($\mathbf{T}_{I\times N}$) and two loading matrices are returned, one for the (relaxation) time mode ($\mathbf{P}_{M\times N}$) and one for the *slab* mode ($\mathbf{S}_{K\times N}$), where N is the number of components resolved. Figure 3 shows the elements resulting from the trilinear decomposition of the three-way array plus a residual array. As a consequence of the lagging procedure the time mode loadings ($\mathbf{P}_{\text{red}}$) will only contain the intersection information and thus not be of full length compared with the acquired data. In step 3 full-length time mode loadings ($\mathbf{P}_{\text{full}}$) are restored using a least squares regression of the raw data onto the estimated amplitudes, $\mathbf{T}$,

$$\mathbf{P}_{\text{full}} = (\mathbf{T}^{+} \cdot \mathbf{X})^{\text{T}}, \qquad [6]$$

where $\mathbf{T}^{+}$ is the pseudo inverse of $\mathbf{T}$. This algorithmic step is not strictly necessary but is performed to conserve the original data structure. Once $\mathbf{P}_{\text{full}}$ has been found each of the N full-length loadings (columns of $\mathbf{P}_{\text{full}}$) are individually monoexponentially fitted (*9*), in step 4, to ensure that the relaxation profiles are in accordance with the model in Eq. [1]. The monoexponential fitting is a robust and fast calculation and the fitted time constants and amplitudes are used to reconstruct (step 5) new pure full-length monoexponential loadings ($\mathbf{P}_{\text{exp}}$), so that $\mathbf{P}_{\text{full}} = \mathbf{P}_{\text{exp}} + \mathbf{E}_{\text{exp}}$. The scores that correspond to the pure exponential loadings can be calculated from the raw data as

$$\mathbf{T}_{\text{exp}} = \mathbf{X} \cdot \left(\mathbf{P}_{\text{exp}}^{\text{T}}\right)^{+}. \qquad [7]$$

Steps 4 and 5 can be considered to be guard steps which are performed (a) to ensure that the calculated scores (concentrations) only relate to pure exponentials, (b) because a comparison between the DTLD loadings and the SLICING loadings (monoexponentials) can be used as a diagnostic tool, and (c) to simultaneously determine the characteristic T_2 relaxation times.

Finally, in step 6 the model error of the SLICING fit can be calculated as the squared sum of errors (SSE),

$$\text{SSE} = \left\|\mathbf{X} - \mathbf{T}_{\text{exp}} \cdot \mathbf{P}_{\text{exp}}^{\text{T}}\right\|_F^2, \qquad [8]$$

where subscript F implies the Frobenius norm. It is noteworthy that neither the initial DTLD solution or the final solution above provides least squares fit. However, if the assumptions behind Eq. [3] are valid, the deviation from the least squares solution is expected to be insignificant. To obtain an estimate of the model error which is independent of the number of components extracted, the SSE must be divided by the degrees of freedom to yield the mean squared error (MSE). It is no trivial matter to determine the degrees of freedom in a three-way problem, even more so in this case, where the three-way solution has been transformed through sequential reestimation in terms of the original two-way data. A reasonable approximation is to correct for the number of elements minus the number of parameters used. The error corrected for degrees of freedom can thus be calculated as

$$\text{MSE} = \frac{\text{SSE}}{I \cdot J - N \cdot (I + J)}. \qquad [9]$$

For each SLICING scheme, steps 1 to 6 must be repeated for a range of components, N, and the results compared through the MSE in order to find the optimal N. If the $\text{SLICING}_{\text{OPT}}$ model is to be calculated, steps 1 to 6 are to be repeated for a range of all three metaparameters *lag, slab*, and N in order to find the optimal model. The final outcome of such exhaustive calculation is a *lag-slab*-diagram which holds the SSE landscape of SLICING performance (Fig. 4)—the minimum value is the $\text{SLICING}_{\text{OPT}}$ model for a given N. In general such a plot reveals typically a complex discontinuous landscape with a trend for interdependence between the optimal choice of *lag* and *slab* and where large regions of combinations of *lag* and *slab* have practically identical SSE values.

The outlined SLICING algorithm has proven a robust method for determining the dimension of the system compared to just examining the DTLD error. Through the pure monoexponential loadings, the T_2 values of the system components are determined simultaneously. In preliminary simulations no significant differences in algorithmic performance were found between full length scores, exponential scores, and DTLD scores, as well as between PARAFAC and DTLD calculations.

Principal Phase Correction

Typically LF-NMR quadrature data are magnitude transformed to correct for phase errors in the acquisition. This procedure represents a simple and robust transformation independent of detection of phase angle and can mathematically be described as in Eq. [10]. Here the two quadrature data channels have been named **a** and **b**, and letting **x** be the transformed intensity data then the magnitude transformation can be written as

$$\mathbf{x}_{\text{magnitude}} = \sqrt{\mathbf{a}^2 + \mathbf{b}^2}. \qquad [10]$$

This transformation does not allow negative values which is a problem, especially for high noise level data, when the system has been allowed to relax to zero intensity. This introduces a bias in terms of nonexponentiality in the magnitude corrected data that poses a problem since all algorithms based on Eq. [1] require underlying exponential structures.

The solution to the problem is to phase-rotate the acquired quadrature data since negative values are allowed and no artifacts thus introduced. Van der Weerd *et al.* (*28*) discussed this problem of using magnitude-transformed data and proposed an algorithm for phase rotation of the quadrature data. For their

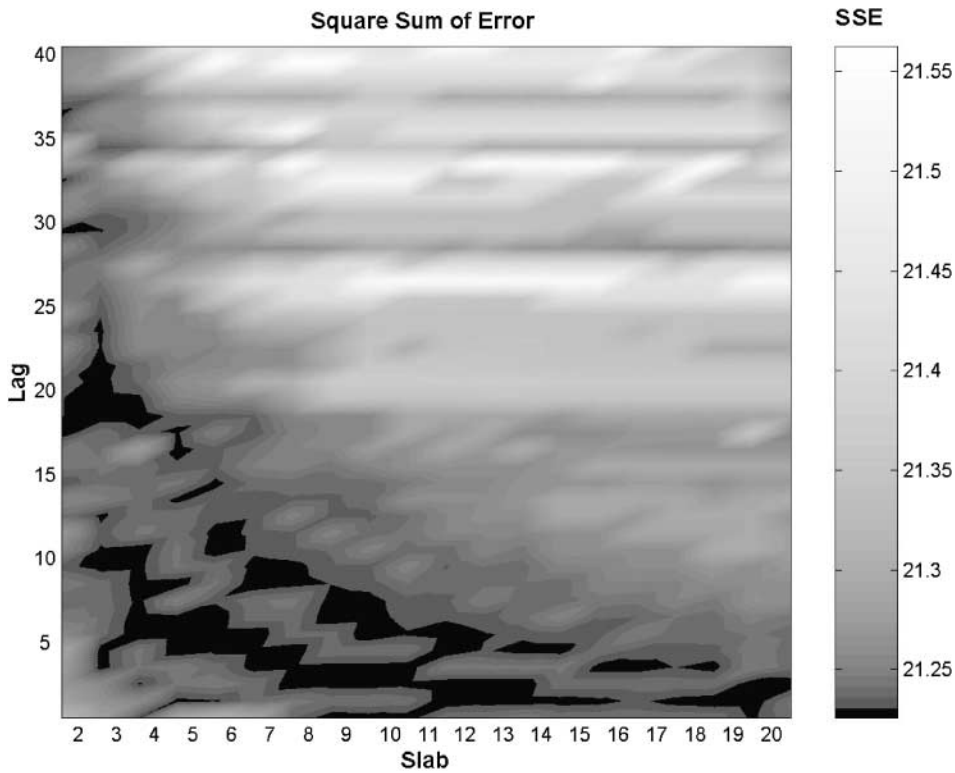

FIG. 4. *Lag* and *slab* diagram for SLICING$_{OPT}$ displaying the SSE as a function of the *lag* and *slab* metaparameters.

proposed method to work it is mandatory that the phase angle for each sample be known which may be a problem particularly if the phase drifts during acquisition. In this work we propose a new, simple, and noniterative procedure for performing phase correction for LF-NMR CPMG data called Principal Phase Correction (PPC) which is based on singular value decomposition (*29*). PPC is independent of storing phase angles and applicable to most quadrature data and it has the advantage of also filtering away possible noise in the individual measurements. Again **a** and **b** are two *J*-vectors holding the two quadrature channels. Then PPC-rotation is performed by a singular value decomposition (SVD). Ideally, the second singular value is zero if there are no changes in phase throughout the measurements. In practice though, minor differences are observed and the second singular component represents this noise as explained, e.g., by Malinowski (*30*). The product of the first left singular vector times the first singular value provides an optimal representation of the phase rotated measurements and the influence of noise is reduced.

Experimental Design

In order to test the robustness of the different algorithms evaluated in this paper an experimental design was carried out where a total of seven variables were varied: the number of components, the number of data points in the profiles, the distance between the T_2 times of the components, the correlation between concentration profiles (CORR), the uncorrected corrrelation between profiles (UCC), number of samples in the datasets, and noise, all of which are expected to be influential for how difficult it is to estimate the underlying parameters accurately. The correlation between profiles is a standard measure for expressing similarity. However, as the data are usually not centered, correlations can be misleading. For example, two profiles, could in principle have a perfect correlation but be very different because of a possible offset in one of the profiles. The uncorrected correlation coefficient (or Tuckers congruence coefficient) (*31, 32*) is a measure similar to the correlation which does take the offsets into account. It is defined as

$$\varphi(\mathbf{x}, \mathbf{y}) = \frac{\mathbf{x}'\mathbf{y}}{\sqrt{\mathbf{x}'\mathbf{x}}\sqrt{\mathbf{y}'\mathbf{y}}} \qquad [11]$$

and is hence a number between -1 and 1. The closer to one, the more similar the two vectors are. The experiment was performed as a full factorial design with each variable at two levels—high/low—and for each design point, 10 replicates were made, each replicate based on a new set of scores and new white noise of the desired level.

The ability of the different algorithms to deconvolute the time constants used to construct the data sets is evaluated such that if one or more deconvoluted time constants deviate more than a specified limit (e.g., 50%) from the known value, the entire

solution is said to be erroneous. This way the robustness of the algorithms is not evaluated based on the absolute value of SSE of the solutions but rather on logic basis: acceptable or not acceptable. Within the acceptable region, though, a more quantitative analysis of the results is given.

RESULTS AND DISCUSSION

When working with multiway multivariate data analysis it is easy to be exalted by the beauty of the SLICING approach. Without asking explicitly for exponential loadings the basically noniterative algorithm yields near-perfect monoexponential loadings which on top are unique solutions in the mathematically sense. This would appear to be an extraordinarily sound and healthy property of a multiexponential fitting algorithm, but it must be stressed that the exponential behavior is implicitly built into the algorithm per construction and moreover the determination of the number of components to resolve was not all that unequivocal in practice.

Before praising a new algorithm, its performance must be compared to existing related algorithms, which is the purpose of the following thorough performance test. Initial performance tests failed to indicate that the performance of the SLICING algorithm was equal to the MATRIXFIT algorithm. An example of such an intitial test is given in Fig. 5 in which the T_2 dispersion for 3000 replicate simulations with random noise is displayed. The figure clearly indicates a narrower distribution for the $\text{SLICING}_{\text{OPT}}$ than for the DECRA; however, the T_2 dispersion for the MATRIXFIT algorithm was markedly better. For these reasons a large scale experimental design with simulated data was set up in order to investigate in depth if the SLICING was always performing inferior to the MATRIXFIT algorithm considering all possible combinations of variables related to its application including number of components, noise level, time separation of components, intercorrelation levels, etc.

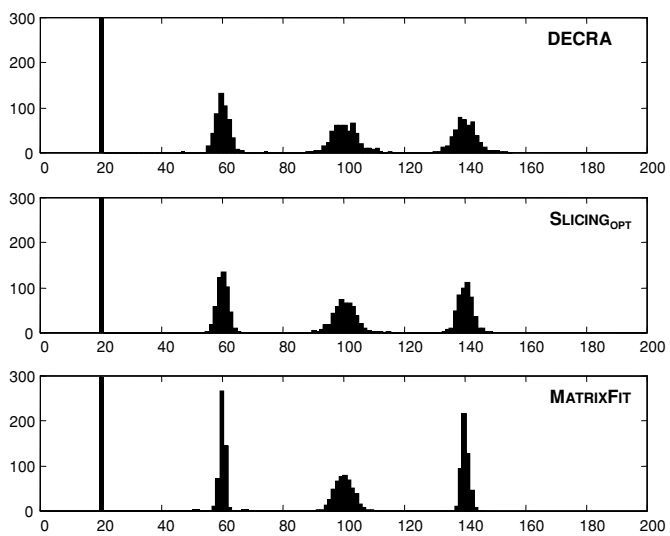

FIG. 5. Bar graph displaying the distribution of T_2 values as a function of the 2D curve fitting algorithm used: DECRA, $\text{SLICING}_{\text{OPT}}$, and MATRIXFIT. This preliminary algorithm test was performed with 3000 replicates on simulated data from 30 samples with 4 components and 200 data points. The data were added 0.1% random noise and the magnitudes were only correlated with a coefficient of 0.3.

TABLE 1
Design Variables Used in the Experimental Design along with the Levels Used for the Different Factors

Factor	Low	High
Correlation	0.5	0.95
Time distance between components	2	4
Noise (%)	0.5	5
Number of components	2	5
Number of data points	16	512
Number of samples in data set	10	30
UCC	0.5	0.95

Application 1: Simulated Data

In practice, it is impossible to produce artificial data that genuinely behave as real data. Therefore, work performed on simulated data is at most to be considered as an ideal and limiting case. However, it is instructive to analyze artificial data, because complete knowledge of the data makes it possible to precisely investigate the quality of the solutions. In this section the results of the experimental design will be discussed.

The different design factors and the values are listed in Table 1. Since the number of components, N, and the difference between these components' relaxation times influence the endpoints of the time axis if proper description of data is to be obtained, different time axes were created to ensure good description for all design points. Also, since some of the algorithms examined can only be applied with a sufficiently large number of variables, only three algorithms are tested with the low number of data points. These are MATRIXFIT, DECRA, and $\text{SLICING}_{\text{OPT}}$. Thus two separate data analyses had to be performed depending on the number of data points in the profiles. When performing a full factorial design with 7 variables, each at 2 levels, a total of 128 experiments can be performed. Since 10 replicates were performed for each design point a total of 1280 data sets were generated and analyzed either by 3 or 7 different algorithms depending on the number of data points in the given design point.

Table 2 lists the success rate of the different algorithms when two different cut-off levels are used: $\pm 50\%$ or $\pm 1\%$ deviation allowed from the known design values, i.e., the set of T_2 values. Clearly the success rate decreases as narrowing the cut-off limit increases the demand for precision. Also it is apparent when comparing the algorithms used for calculation with both 16 and 512 data points that the number of data points describing the data is very important for the robustness of the algorithms. The table reveals that MATRIXFIT is the most robust algorithm followed by $\text{SLICING}_{\text{OPT}}$, and that the robustness for the different

TABLE 2
Total Percentage of Calculated Models Where All Time Constants are within a ±50% Limit (±1% Limit in Brackets)

Algorithm	Data points = 16	Data points = 512
MATRIXFIT	51% (22%)	95% (53%)
DECRA	50% (20%)	78% (28%)
$SLICING_{OPT}$, correlated noise		88% (48%)
$SLICING_{[1\text{-}10\text{-}100;3]}$, correlated noise		73% (39%)
$SLICING_{[1\text{-}5\text{-}10\text{-}50\text{-}100;5]}$, correlated noise		78% (41%)
DECRA, uncorrelated noise	49% (11%)	59% (4%)
$SLICING_{OPT}$, uncorrelated noise		71% (26%)

Note. The total number of calculated models is 640 for each algorithm.

SLICING approaches is improved when using more than two *slabs*.

Figure 6A shows a boxplot indicating the spread of the calculated solutions for the different algorithms used in the study. Only plots for the results with 512 data points in the data sets as well as the solution with a cut-off value of ±50% are shown. Since the success rate of the different algorithms varies, it was decided to include only the solutions that are found to be good (within the cut-off limit) for all seven algorithms. Moreover, some of the algorithm indicators in the boxplot are compressed due to a much larger spread for other algorithms; the plot has been reproduced with only the three main algorithms (Fig. 6B) which reveal a much larger spread for DECRA than for the other

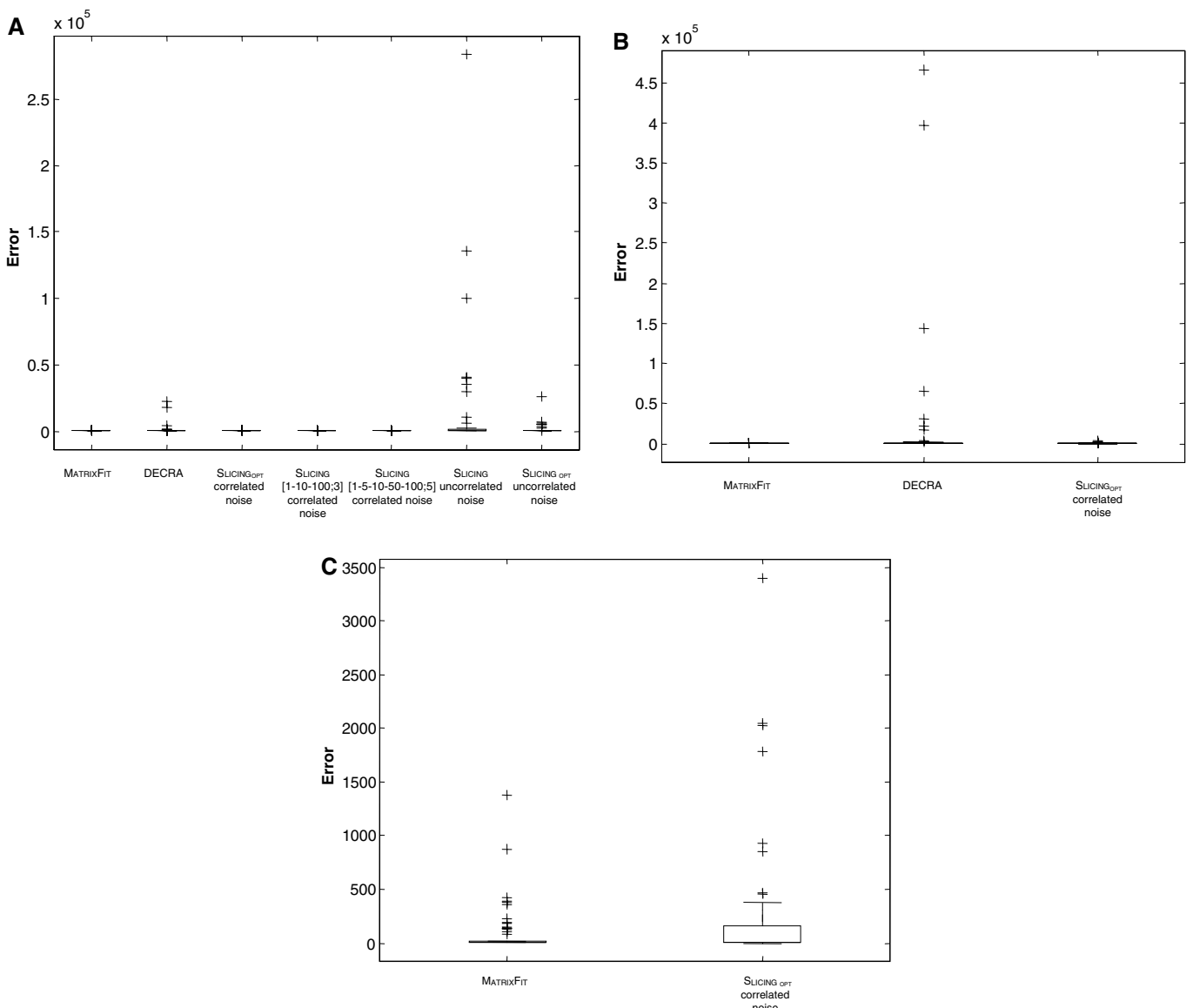

FIG. 6. Box plots comparing the experimental design solutions for all investigated algorithms.

TABLE 3
Time Consumption in Seconds upon Fitting from Two to Five Components in Simulated Data Sets Where the Number of Samples (25 or 100) and the Number of Variables (256 or 1024) Have Been Varied in Two Levels

	Components	2		3		4		5	
	Variables								
	Samples	256	1024	256	1024	256	1024	256	1024
Exponential fit	25	2.1	5.2	5.5	11.1	8.5	23.4	21.3	50.1
	100	8.9	19.3	18.2	43.2	54.0	96.1	81.0	184.1
MATRIXFIT	25	0.2	0.5	0.4	1.8	0.7	3.6	1.4	4.7
	100	1.0	5.4	1.7	7.9	2.6	13.7	4.6	22.5
DECRA/SLICING$_{OPT}$[a]	25	0.05	0.1	0.06	0.3	0.07	0.3	0.08	0.45
	100	0.09	3.2	0.15	3.3	0.15	3.8	0.14	4.4

[a] Since calculations of the DECRA and the individual SLICING$_{OPT}$ models are based on the same algorithm (only varying in the degree of "slicing") these share calculation time.

two algorithms. In Fig. 6C only MATRIXFIT and SLICING$_{OPT}$ (with correlated noise) are compared. Once the number of algorithms included in the boxplot is reduced, the number of good solutions included in the boxplot increases due to the fact that the highlighted methods represent the more robust approaches applied.

Based on this experimental design of simulated data it is clear that in terms of deconvolution of the time constants the SLICING$_{OPT}$ produce more consistent deconvolution than DECRA, and that MATRIXFIT perform slightly better than SLICING$_{OPT}$. This result basically confirms the initial performance test described above. Concerning the importance of the different design parameters it was found that the number of T_2 components and the noise level were the most important design parameters regardless of the number of variables in the profiles. The importance of all design variables (excluding the number of variables) in terms of robustness to extract T_2 components is listed in order of priority below:

- 16 variable: factors > noise > correlation > samples > distance > UCC
- 512 variable: factors > noise > UCC > correlation > samples > distance.

It is noteworthy that the distance between the T_2 components did not come out as a most important design factor. A second remarkable observation (Table 2) is the fact that the number of variables in the simulated profiles is a very important parameter for proper description and deconvolution of the underlying T_2 components. Clearly not all design parameters are important when evaluated individually; however, when combined with other main effects they may become quite important. The SLICING approach based on uncorrelated noise was found to perform significantly poorer than its counterparts based on the normal slicing approach. The rationale behind this approach of improving the SLICING approach by generating slices without redundant information and thus without correlated noise was clearly wrong. The reason for this result remains to be elucidated.

Since speed of calculation is an important issue, 4 different data sets were generated (using the same approach as for the experimental design) based on 2 to 5 components. All 4 data sets were generated with 100 samples and 1024 variables (time points) and calculations on the reduced sets were performed on a subset of these data sets. In Table 3 the performance of the main algorithms can be compared in terms of the times required to fit the different data sets. Both the number of samples as well as the number of variables in a data set influence the time of consumption, with the 1D exponential fit being more dependent on the number of samples and the 2D methods being more dependent on the number of variables (albeit almost negligible). For the 2D methods the prime importance is the total number of variables present in the data set. These observations were expected since for the 1D exponential fitting the fit is calculated for one sample at the time, obviously giving strong dependence on the number of samples, whereas for the 2D methods all samples were treated simultaneously. Clearly, 1D exponential fitting is by far the most time consuming process with MATRIXFIT, although still iterative, being much faster while the direct noniterative approach of DECRA/SLICING$_{OPT}$ by far being the fastest approach for deconvolution of the underlying time constants. An increase in algorithmic speed of the multiexponential fitting procedure (Simplex search (*33*)) is indeed possible, but according to our experience the increase is only minimal with other more sophisticated line search methods and far from a speed comparable to that of the SLICING algorithm.

Application 2: Fat Content in Minced Meat

This data set consists of measurements on 47 samples of minced meat with a total fat content ranging from 1.2% to 15% (w/w). A multivariate upgrade of the pulsed field gradient stimulated echo experiment (*34*) was used. In this experiment, called diffusion-CPMG (DIFF-CPMG), the standard pulsed field gradient stimulated echo experiment is followed by a 180° pulse train, as seen in the CPMG experiment. The original purpose of this experiment was to improve the standard univariate pulse field gradient method for total fat prediction by

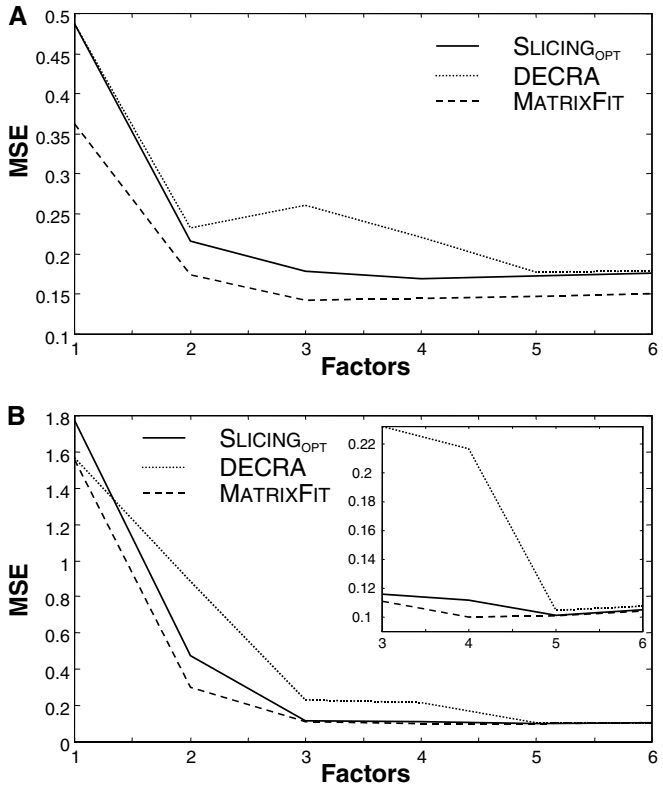

FIG. 7. MSE residual plot as the optimal SLICING solution as a function of the number of components present in the real data sets: (A) fat content in minced meat and (B) preslaughter stress.

application of a more robust bilinear multivariate approach using partial least squares (PLS) regression (*35*). The samples were equilibrated at 55°C for 30 minutes before analysis to ensure liquid fat phase, and a total of 2048 even echoes were acquired with a τ of 500 μs. Besides analyzing these data by traditional multiexponential fitting, data were also analyzed by means of MATRIXFIT, DECRA, and SLICING$_{OPT}$. The results of these four algorithms are presented in the following.

On this real data set the 1D multiexponential fitting appears only to support 2 components as evaluated by the decrease in the residual norm. For MATRIXFIT 3 components appear to be the optimal choice. Using the SLICING approach the optimal model was found for a 4-component system ($lag = 20$; $slab = 4$) as indicated in the MSE plot in Fig. 7A. In this case the development in the MSE of the DECRA model displayed a peculiar trend with a maximum at the 4-component solution and no optimal solution within 6-components. Figure 8 shows a plot of the SLICING$_{OPT}$ loadings when extracting 1 to 6 components. The corresponding time constants and MSEs of the models are also provided. While the 1- to 5-component SLICING models generate visually sound loadings, the 6-component SLICING model appears not to be a valid solution. Examination of the 5-component solution reveals that 2 of the corresponding DTLD loadings display nonexponential behavior and have significantly increased noise levels, which is a typical result when an attempt is made to resolve too many components by the SLICING algorithm. When a 6th component is extracted a negative clearly nonexponential DTLD loading is the result. Based on these findings, and since the 4-component model based on $lag = 20$ and $slab = 4$ gives the smallest MSE, it can be concluded that there are a maximum of 4 relaxation components in the system. In this application, having a quantitative purpose, the performance of the different algorithms is compared in the following three steps:

(I) The best-correlating single component concentration (M_x) vector resulting from either exponential fit or the mentioned two-dimensional algorithms is used for univariate linear regression prediction of the total fat content. The component that gives the best univariate linear regression model is assumed to represent the fat protons.

(II) All concentration vectors resulting from either exponential fit or the mentioned two-dimensional algorithms are used for predicting total fat content using multiple linear regression models.

(III) Entire relaxation decays are used for PLS models, predicting fat content, and the results are compared to the results obtained by univariate and multiple linear regression using scores (concentrations) obtained from the different algorithms. This is the pragmatic and efficient "model-free" approach, which only suffers from near-orthogonal loadings that cannot be easily interpreted. It is normally to be expected that the best regression results are obtained with PLS, for which reason the comparison is mainly interesting, because it provides an impression of how close calibration based on the two-dimensional algorithms comes to the results obtained with PLS.

The proton component with the time constant T_{22} ranging from 234 to 318 ms from the biexponential fitting displayed a strong covariation with the fat content of the samples. With MATRIXFIT the best correlation for a 3-component model is obtained using T_{23} with a time constant of 463 ms and similarly for 4-component DECRA and SLICING$_{OPT}$ solutions, a T_{23} of 246 and 253 ms, respectively, yields the best models. In Table 4 univariate linear regressions based on these concentration vectors are compared based on the correlation coefficient (r) and a root mean square of cross validation (RMSECV). For comparison, a simple DIFF-CPMG measurement of beef lard at 55°C yielded

TABLE 4

Performance of Prediction of Fat Content for the Different Main Algorithms When Only the Concentration Vector Best Modelling the Fat Content is Used

Algorithm	T_{2x} (ms)	# PC	r	RMSECV % (w/w fat)
Multiexponential fit	234–318	2	0.98	0.63
MATRIXFIT	463	3	0.99	0.57
DECRA	246	4	0.99	0.57
SLICING$_{OPT}$	253	4	0.99	0.55

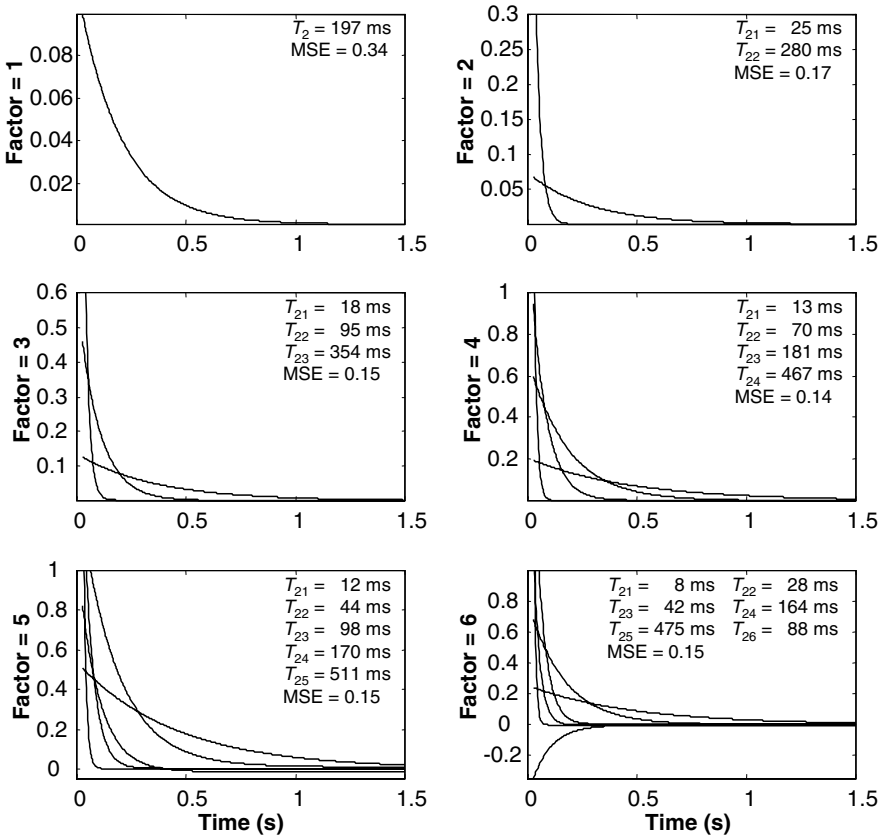

FIG. 8. Plot of the SLICING loadings from the fat in the meat data set when extracting one to six components, including time constants and MSE of the models. The axes have been changed to enlarge the interesting part of the loadings. Models based on one to four components clearly generate good loadings, whereas the 5- and 6-component models are not good solutions. Apparently the 4-component solution is the best model, resulting in the smallest MSE.

no less than three T_2 components (75, 186, and 480 ms) of which the middle component is in fair agreement with the T_{23} component of SLICING$_{OPT}$ and DECRA models whereas the third component is in good agreement with T_{33} of the MATRIXFIT solution.

For the biexponential fit, inclusion of both concentration (amplitude) vectors from the biexponential fit in a multiple linear regression model did not improve the univariate prediction mentioned above. For the other two-dimensional methods, however, the multiple linear regression model built on all the scores (concentrations) from the 3- or 4-component models, respectively, resulted in a significantly improved prediction model. The performances of these optimal models are compared in Table 5. If the predictive performance for the three algorithms based on three to five components is compared (Tabel 5) it appears that there is only minor differences between these. It appears that selection of the number of components to use is not too critical as long as it is within a limited range of the correct number and all concentrations are used rather than calculating univariate models based on a single concentration vector.

For comparison the PLS model using the entire relaxation data yielded a two PLS component solution with a correlation coefficient of $r = 0.99$ and a prediction error of RMSECV = 0.49% (w/w fat). Thus, in this data set the higher-order deconvolution methods based on exponentiality perform as well as the PLS model.

Application 3: Preslaughter Stress in Processed Meat

Classification of slaughtered pig carcasses according to their "stress treatment" may be an informative quality parameter, as stress will influence the meat quality after slaughter. This data set

TABLE 5

Predictive Performance for Fat in Meat When Using Scores Calculated by MATRIXFIT, DECRA, and SLICING$_{OPT}$ for Different Number of Components

Algorithm	# PC	Correlation	RMSECV
MATRIXFIT	3	0.99	0.47
DECRA	4	0.99	0.47
SLICING$_{OPT}$	4	0.99	0.48

Note. For all the listed models all scores are used for the prediction.

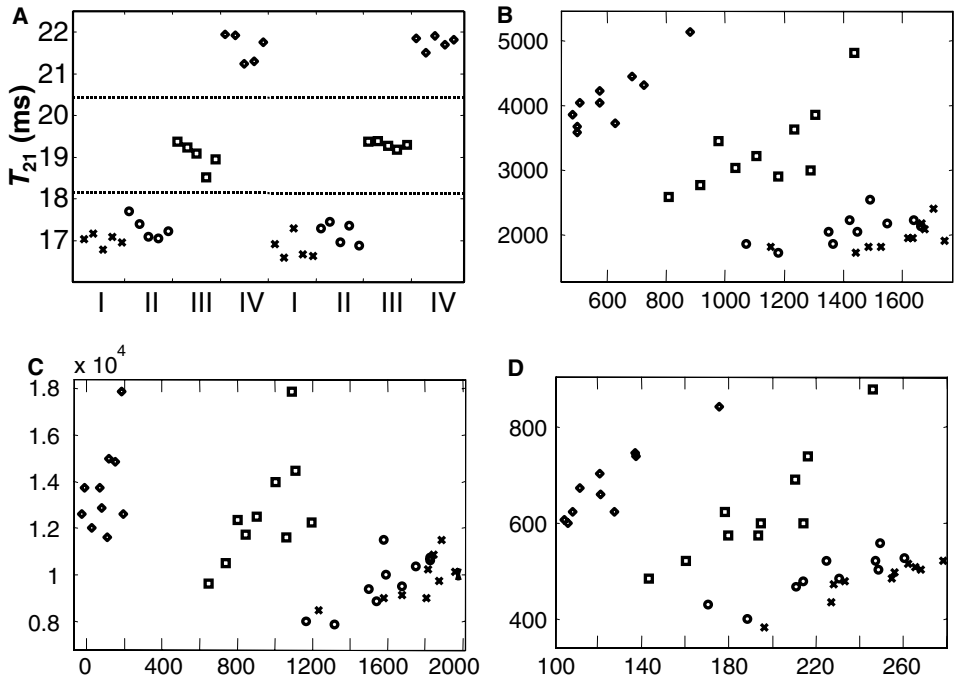

FIG. 9. (A) Stress groups (I, II, III and IV) plotted versus T_{21} from a bi-exponential fit. The two "subgroups" each including (I, II, III, IV) represent the two long sides of the pig. (B, C and D) are scatter plots of the scores of T_{22} versus the scores of T_{23} for a five-component two-dimensional model: (B) MATRIXFIT, (C) DECRA and (D) SLICING$_{OPT}$.

consists of CPMG relaxation profiles from 40 porcine meat samples and is used to test the strength of SLICING in a classification problem. The relaxation data have been measured on processed meat taken from *Musculus semimembranosus* from pigs stressed at four different levels: (I) control, minimum stress prior to slaughter, (II) pigs running on a treadmill for 10 minutes prior to slaughter, (III) pigs injected with epinephrine 15 h prior to slaughter, and (IV) pigs injected with epinephrine 15 h prior to slaughter and running on a treadmill for 5 minute prior to slaughter. The data were originally acquired in an experiment conducted to analyze for warmed over flavor (WOF), and the samples had therefore been boiled in sealed plastic bags and then analyzed the following days (*35*).

Using multiexponential fitting, only two components seemed to be supported by the relaxation data of the processed meat samples as evaluated by the reduction in the residual error. Figure 9A shows a plot of the short time constant, T_{21}, from the biexponential fitting as a function of the stress level group. The plot demonstrates a clear visible grouping among the stress level groups. Only the treatments I and II cannot clearly be separated. This result is in itself significant. NMR measures a change in the states of the water protons and therefore in the muscle structure caused by preslaughter stress which is pertinent to the slaughter, rigor development, and processing. It is surprising that such a clear effect of stress can be detected with animals which are less stressed than at commercial slaughterhouses. That the control pig (I) and stress treatment (II) could not be separated was confirmed by biochemical indicators. The long time constant, T_{22}, ranging from 55 to 63 ms was found to be relatively constant and insensitive to the level of preslaughter stress.

The results from the biexponential fit indicate that this data set may not represent the ideal situation for application of the higher order methods, because the samples are differentiated based on their change in time constants rather than on the concentrations of common time constants, as was the case in application 2. However, since the algorithms allow components to have zero concentration, extraction of components being present in some samples but not in others is possible.

From the results obtained in the one-dimensional biexponential fitting it might seem logical to expect the optimal SLICING solution to be a 4-component solution: one component for T_{22} which was fairly constant for all samples and 3 components for the 3 separable stress levels reflected by T_{21} in the biexponential fit. This is, however, not what we found. When the SLICING models were calculated, the combination of $lag = 6$ and $slab = 2$ using five components (0.8, 11, 25, 31, and 75 ms) resulted in the smallest MSE as also indicated in the MSE residual plot in Fig. 7B. As indicated by the figure, a 5-component model was also found by the ($lag = 1$; $slab = 2$)-model (0.3, 8, 20, 39, and 83 ms) as well as for MATRIXFIT (0.9, 12, 25, 45, and 103 ms). Interestingly none of the time constants of the biexponential fitting is recovered in any of the 5-component two-dimensional solutions wherefore one or both of the underlying physical models must be erroneous. Comparing all four subplots in Fig. 9 it

appears that there is only minor variation between the groupings in the different subplots reflecting similar ability to extract the information known to be present in the data set.

CONCLUSIONS

The SLICING method outlined in this study is an *elegant* alternative method based on trilinear decomposition for performing two-dimensional multiexponential fitting of LF-NMR time domain relaxation data. The advantage of the SLICING method is that the solutions are analytical and that no initial value guesses are required. Despite the apparent complexity of the SLICING method the noniterative character makes the method highly performant and this study reveals a substantial speed advantage when compared to a traditional iterative curve fitting method. Moreover the computational complexity is independent of the number of components to be resolved.

Even though the SLICING algorithm is unique and provides estimates of the underlying T_2-components, it is not a fully automated procedure. It is necessary that the number of components be chosen correctly because the estimated T_2-values vary with the number of components chosen. However, the SLICING algorithm includes improved diagnostics for determining the number of T_2-components. In the test examples described here and in other applications we have tested thus far, SLICING tends to produce clearly unrealistic and/or insignificant relaxation components if the number of components is set too large and is therefore a better probe for system dimensions (number of proton components) than any other algorithmic approach we have tested. In this study a number of different schemes for trilinear upgrade of the multiexponential relaxation decays is tested and compared. The SLICING algorithm proved to be only mildly sensitive to the two metaparameters, *lag* and *slab*, while a new original slicing scheme with uncorrelated noise (nonredundant *slab* information) surprisingly appeared to deteriorate the performance. The simplest possible slicing scheme with *lag* equal to one and slab equal to two (as in the original DECRA algorithm) proved to not be optimal in terms of explained variance but in practice almost equally well as a more elaborate and time consuming optimal SLICING approach.

At an early stage the SLICING algorithm in some cases proved to be adversely influenced by the use of magnitude data. For this reason a new phase rotation method, principal phase correction, based on SVD was devised for conversion of quadrature data without knowledge of the phase angle. This method is generally applicable and not specifically related to the SLICING algorithm.

At the bottom line, SLICING is an outmost efficient algorithm for two-dimensional analysis of time-domain LF-NMR signals which performs almost equally as well as its numerical brother algorithms. For this reason we predict an important future for the SLICING algorithm as a preprocessing tool to provide highly qualified guesses for robust traditional curve fitting algorithms. However, in two-dimensional applications where the number of samples is low SLICING might be the only alternative as it brings the additional advantage that calibration to reference measurements referring to individual proton components require only simple scaling of SLICING scores.

EXPERIMENTAL

All data were acquired using a MARAN low-field bench-top instrument (Resonance Instruments, Witney, UK) equipped with a 23.2-MHz high-quality permanent magnet and using an 18-mm variable temperature gradient probe. Handling of data and all subsequent analysis were performed in MATLAB v. 5.3 (MathWorks Inc., Natic, USA) on a portable PC equipped with a PIII 900-MHz processor, 256 MB RAM running Windows 2000. Both one-dimensional and two-dimensional exponential fitting were performed with an algorithm written in house, based on a Simplex minimization of the nonlinear parameters and a least squares estimation of the linear parameters inside the function evaluation call (*9*) (Pedersen and Engelsen, www.models.kvl.dk/source/lfnmr). The *Direct TriLinear Decomposition* (DTLD) algorithm applied was from the N-way Toolbox v. 1.03 for MATLAB (Andersson and Bro, www.models.kvl.dk/source/nway). The SLICING algorithm is available from Pedersen, Bro, and Engelsen, www.models.kvl.dk/source/lfnmr.

ACKNOWLEDGMENTS

We thank Gilda Kischinovsky for helpful editing of the manuscript. The Danish Veterinary and Agricultural Research Council (SJVF) are acknowledged for supporting Ph.D. student Henrik Toft Pedersen through the funding of The Centre for Critical Quality Attribute Determination in Muscle Foods. The Centre for Predictive Multivariate Process Analysis is acknowledged for funding of the NMR equipment. R. Bro thanks frame program AQM (Advanced Quality Monitoring in the Food Production Chain), as well as STVF project Mathematical models for multi-way Data for financial support.

REFERENCES

1. W. Windig and B. Antalek, Direct exponential curve resolution algorithm (DECRA): A novel application of the generalized rank annihilation method for a single spectral mixture data set with exponentially decaying contribution profiles, *Chemom. Intell. Lab. Syst.* **37,** 241–254 (1997).
2. J. G. Diegel and M. M. Pintar, Origin of the nonexponentiallity of the water proton spin relaxations in tissues, *Biophys. J.* **15,** 855–860 (1975).
3. M. Köpf, C. Corinth, O. Haferkamp, and T. F. Nonnenmacher, Anomalous diffusion of water in biological tissues, *Biophys. J.* **70,** 2950–2958 (1996).
4. R. Prony, Essai Expérimental et Analytique sur les Lois de la Dilatibilité et sur celles de la Force Expansive de la Vapeur de l'Eau et de la Vapeur de l'Alkool, a Différentes Températures, *J. Ecole Polytech.* **1,** 24–76 (1795).
5. J. P. Butler, J. A. Reeds, and S. V. Dawson, Estimating solutions of first kind integral equations with nonnegative constraints and optimal smoothing, *SIAM J. Numer. Anal.* **18,** 381–397 (1981).
6. S. W. Provencher, CONTIN: A general purpose constrained regularization program for inverting noisy linear algebraic and integral equations, *Comp. Phys. Comm.* **27,** 229–242 (1982).

7. L. G. Thygesen, PLS calibration of pulse NMR free induction decay for determining moisture content and basic density of softwood above fiber saturation, *Holzforschung* **50,** 434–436 (1996).
8. A. Gerbanowski, D. N. Rutledge, M. H. Feinberg, and C. J. Ducauze, Multivariate regression applied to time domain nuclear magnetic resonance signals: Determination of moisture in meat products, *Sci. Aliment.* **17,** 309–323 (1997).
9. I. E. Bechmann, H. T. Pedersen, L. Nørgaard, and S. B. Engelsen, Comparative chemometric analysis of transverse low-field ^{1}H NMR relaxation data, *in* "Advances in Magnetic Resonance in Food Science" (P. S. Belton, B. P. Hills, and G. A. Webb, Eds.), pp. 217–225, The Royal Society of Chemistry, Cambridge, UK (1999).
10. R. J. S. Brown, F. Capozzi, C. Cavani, M. A. Cremonini, M. Petracci, and G. Placucci, Relationships between H-1 NMR relaxation data and some technological parameters of meat: A chemometric approach, *J. Magn. Reson.* **147,** 89–94 (2000).
11. R. Roy and T. Kailath, Estimation of signal parameters via rotational invariance techniques, *IEEE ASSP Mag.* **37,** 984–995 (1989).
12. M. Viberg, Sensor array processing based on subspace fitting, *IEEE Trans. Signal Process.* **39,** 1110–1121 (1991).
13. N. D. Sidiropoulos, R. Bro, and G. B. Giannakis, Parallel factor analysis in sensor array processing, *IEEE Trans. Signal Process.* **48,** 2377–2388 (2000).
14. W. Windig, J. P. Hornak, and B. Antalek, Multivariate image analysis of magnetic resonance images with the direct exponential curve resolution algorithm (DECRA). Part 1. Algorithm and model study, *J. Magn. Reson.* **132,** 298–306 (1998).
15. B. Antalek, J. P. Hornak, and W. Windig, Multivariate image analysis of magnetic resonance images with the direct exponential curve resolution algorithm (DECRA). Part 2. Application to human brain images, *J. Magn. Reson.* **132,** 307–315 (1998).
16. W. Windig, B. Antalek, L. J. Sorriero, S. Bijlsma, D. J. Louwerse, and A. K. Smilde, Applications and new developments of the direct exponential curve resolution algorithm (DECRA): Examples of spectra and magnetic resonance images, *J. Chemom.* **13,** 95–110 (1999).
17. W. Windig and B. Antalek, Resolving nuclear magnetic resonance data of complex mixtures by three-way methods: Examples of chemical solutions and the human brain, *Chemom. Intell. Lab. Syst.* **46,** 207–219 (1999).
18. S. Bijlsma, D. J. Louwerse, W. Windig, and A. K. Smilde, Rapid estimation of rate constants using on-line SW-NIR and trilinear models, *Anal. Chim. Acta* **376,** 339–355 (1998).
19. S. Bijlsma, D. J. Louwerse, and A. K. Smilde, Estimating rate constants and pure UV-vis spectra of a two-step reaction using trilinear models, *J. Chemom.* **13,** 311–329 (1999).
20. S. Bijlsma and A. K. Smilde, Estimating reaction rate constants from a two-step reaction: A comparison between two-way and three-way methods, *J. Chemom.* **14,** 541–560 (2000).
21. W. Windig, B. Antalek, M. J. Robbins, N. Zumbulyadis, and C. E. Heckler, Applications of the direct exponential curve resolution algorithm (DECRA) to solid state nuclear magnetic resonance and mid-infrared spectra, *J. Chemom.* **14,** 213–227 (2000).
22. R. W. W. van Resandt, R. H. Vogel, and S. W. Provencher, Double beam fluorescence lifetime spectrometer with sub-nanosecond resolution: Application to aqueous tryptophan, *Rev. Sci. Instrum.* **53,** 1392–1397 (1982).
23. R. A. Harshman, Foundations of the PARAFAC procedure: Models and conditions for an 'explanatory' multi-modal factor analysis, *UCLA Working Papers Phonetics* **16,** 1–84 (1970).
24. R. A. Harshman and M. E. Lundy, PARAFAC: Parallel factor analysis, *Comput. Statist. Data Anal.* **18,** 39–72 (1994).
25. R. Bro, PARAFAC: Tutorial and applications, *Chemom. Intell. Lab. Syst.* **38,** 149–171 (1997).
26. E. Sánchez and B. R. Kowalski, Generalized rank annihilation factor analysis, *Anal. Chem.* **58,** 499–501 (1986).
27. E. Sánchez and B. R. Kowalski, Tensorial resolution: A direct trilinear decomposition, *J. Chemom.* **4,** 29–45 (1990).
28. L. van der Weerd, F. J. Vergeldt, P. A. de Jager, and H. Van, As evaluation of algorithms for analysis of NMR relaxation decay curves, *Magn. Reson. Imaging* **18,** 1151–1157 (2000).
29. G. H. Golub and C. F. van Loan, "Matrix Computations," John Hopkins Univ. Press, Baltimore (1989).
30. E. R. Malinowski, "Factor Analysis in Chemistry," Wiley, New York (1991).
31. L. H. Tucker, A method for synthesis of factor analysis studies, Personnel Research Section Report, Dept. of the Army, Report no. **984** (1951).
32. B. C. Mitchell and D. S. Burdick, An empirical comparison of resolution methods for three-way arrays, *Chemom. Intell. Lab. Syst.* **20,** 149–161 (1993).
33. J. A. Nelder and R. Mead, Simplex method for function minimization, *Comput. J.* **7,** 308–313 (1965).
34. H. T. Pedersen, H. Berg, F. Lundby, and S. B. Engelsen, The multivariate advantage in fat determination in meat by Bench-top NMR, *Innov. Food Science Emerg. Tech.* **2,** 87–94 (2001).
35. H. Martens and T. Næs, "Multivariate Calibration," Wiley, New York (1993).
36. J. Brøndum, D. V. Byrne, L. S. Bak, G. Bertelsen, and S. B. Engelsen, Warmed-over flavour in porcine meat—A combined spectroscopic, sensory and chemometric study, *Meat Sci.* **54,** 83–95 (2000).